Rice-Planted Area Detection by Using Self-Organizing Feature Map

Sigeru Omatu

Department of of Electronics, Information, and
Communication Engineering
Osaka Institute of Technology
Osaka, JAPAN 535–8585
Email: omtsgr@gmail.com

Mitsuaki Yano

Department of of Electronics, Information, and
Communication Engineering
Osaka Institute of Technology
Osaka, JAPAN 535–8585
Email: yano@elc.oit.ac.jp

***Abstract*—This paper considers a classification of estimation of rice planted area by using remote sensing data. The classification method is based on a competitive neural network and the sattelite data are remote sensing data observed before and after planting rice in 1999 in Hiroshima, Japan. Three RADAR Satellite (RADARSAT) and one Satellite Pour l'Observation de la Terre(SPOT)/High Resolution Visible (HRV) data are used to extract rice-planted area. Synthetic Aperture Radar (SAR) back-scattering intensity in rice-planted area decreases from April to May and increases from May to June. Thus, three RADARSAT images from April to June are used in this study. The SOM classification was applied the RADARSAT and SPOT to evaluate the rice-planted area estimation. It is shown that the Self-Organizing feature Map (SOM) of competitive neural networks is useful for the classification of the satellite data by SAR to estimate the rice planted area.**

Keywords–Remote Sensing; RADAR Satellite; Synthetic Aperture Radar; Self-Organizing Feature Map

I. INTRODUCTION

We have noticed that rice is the most important agricultural product and widely planted in the wide area in Japan. But, it is still difficult to estimate rice-planted areas every year. Therefore, the development of a system for monitoring the rice crop will be prefarable. Satellite remote sensing images by optical sensors like LANDSAT TM or SPOT HRV, have been used to estimate a rice-planted area. However, these optical sensors have been unable to get necessary data at a suitable time because it is often cloudy or rainy during the rice planting season in Japan [1][2][3][4].

On the other hand, SAR penetrates through the cloud covered. Hence, it can observe the land surface under all weather conditions [5][6][7][8]. The back-scattering intensity of C-band SAR images, such as RADARSAT or ERS1/SAR, changes greatly from non-cultivated bare soil condition before rice planting to inundated condition just after rice planting [1]. In addition, RADARSAT images are rather sensitive to the change of rice biomass in a growing period of rice [9][10].

Thus, a rice area estimation is expected to be achieved in an early stage. In previous works [2][3][4], we attempted to estimate rice-planted area using RADARSAT fine-mode data in an early stage. The estimation accuracy of a rice-planted area by Maximum Lkelihhood Method (MLH) was approximately 40% by comparing with the estimated area by SPOT multi-spectral data. In this study, we attempt to detect the rice-planted area from RADARSAT data using SOM that is the unsupervised classification [11].

In Section II, test site and remote sensing data used here will be explained and in Section III, data correction of geometric distortion will be shown. In Section IV, SOM algorithm will be explained and in Section V, evaluation indexes will be introduced. In Section VI, training results will be shown and in Section VII, selection of training iteration will be discussed. After that, in Section VIII, classification results will be shown and in Section IX, experimental results will be shown. Finally, in Section X, we will conclude the results and state some future aspects.

II. TEST SITE AND DATA

The test area has a size of about 7.5×5.5 km in Higashi-Hiroshima, Japan shown, as a white block in Fig. 1; the enlarged image is shown in Fig. 2. This site is located at the eastern part of Hiroshima, Japan. Three multi-temporal RADARSAT fine-mode (F1F) images, taken on April 8, May 26, and June 19, in 1999 were used as the test data. SPOT/HRV multi- spectral data taken on June 21, 1999 were used to generate a reference image for rice-planted area extraction.

Three merged RADARSAT and one SPOT images in a part of the test site are shown in Figs. 3 and 4. The land surface condition in the rice-planted area of April 8 is a non-cultivated bare soil before rice planting with rather rough soil surface. The surface condition of May 26 is almost smooth water surface just after rice planting, and that of June 19 is a mixed condition of growing rice and water surface. It is found that the rice-planted areas are shown in a dark tone in the RADARSAT image. The RADARSAT raw data were processed using Vexcel SAR Processor (VSARP) and single-look power images with 6.25 meters ground resolution were generated. Then, the images were filtered using median filter with 7×7 moving window. All RADARSAT and SPOT images were overlaid onto the topographic map with 1:25,000 scale. As RADARSAT images are much distorted by foreshortening due to topography, the digital elevation model (DEM) with 50 meters spatial resolution issued by Geographical Survey Institute (GSI) of Japan [2] was used to correct foreshortening of RADARSAT images.

The specifications of RADARSAT-1/SAR fine mode parameters and SPOT-2/HRV parameters are given by Table I and Table II, respectively.

Copyright (c) IARIA, 2014. ISBN: 978-1-61208-354-4

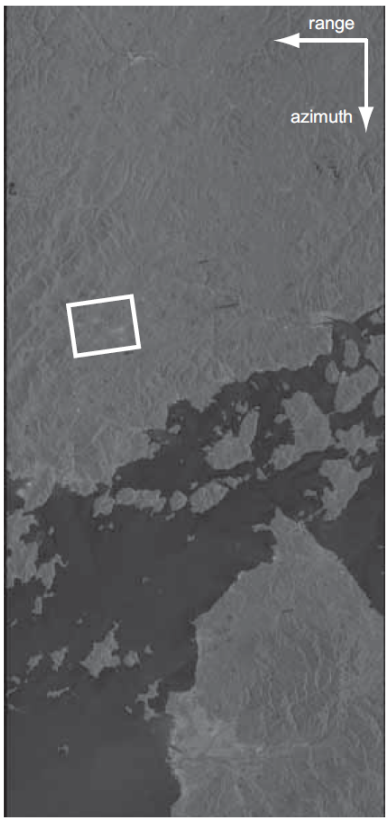

Figure 1. RADARSAT fine mode image of Higashi-Hiroshima, Japan where the area enclosed by a white line denotes the analised area.

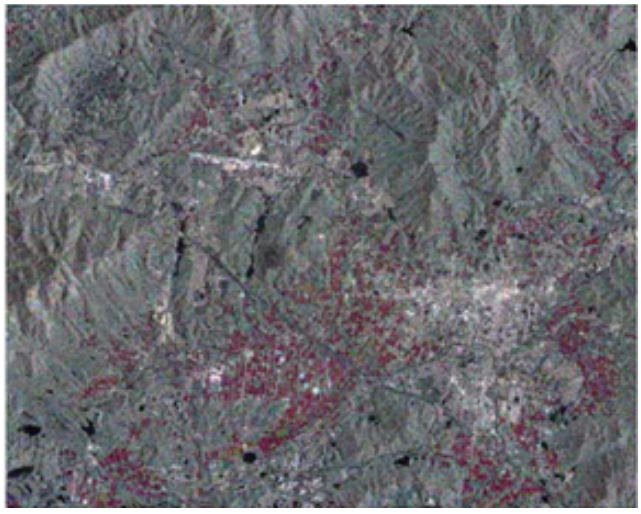

Figure 2. RADARSAT fine mode image of Higashi-Hiroshima where the area enclosed by a white line in Fig. 1 is enlarged..

III. DATA CORRECTION OF GEOMETRIC DISTORTION

SAR or SPOT data observe the land surface from an oblique position as shown in Fig. 5. In Fig. 5, θ denotes incident angles and in case of optical remote sensing data, a deformation D at the height h is given by $D = h \tan\theta$. In case of SAR remote sensing data, it becomes $D = h/\tan\theta$. Therefore, we must correct the remote sensing data according to the hight of the target pixcel. We adopt the mesh data published at GSI of Japan[2].

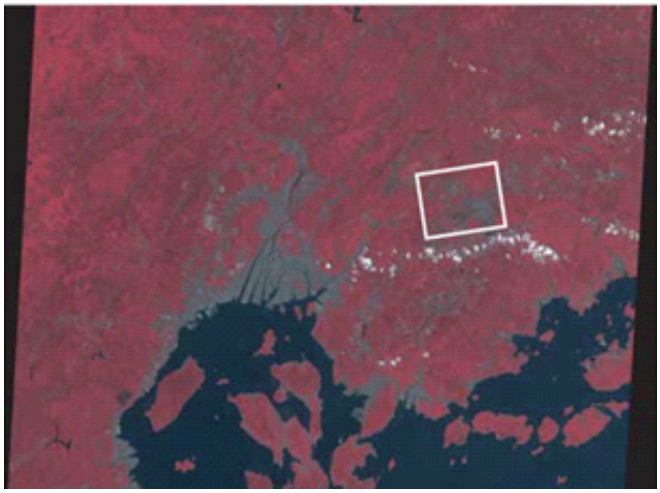

Figure 3. SPOT-2/HRV image(1999/6/21, R:Band 3, G:Band 2, B:Band 1) where the area enclosed by a white line denotes the test area 息 CNESS 1999.

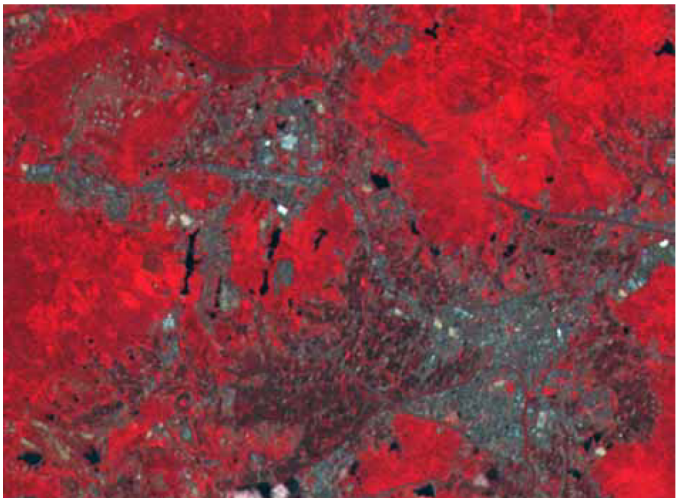

Figure 4. SPOT-2/HRV image(1999/6/21, R:Band 3, G:Band 2, B:Band 1) in the test site 息 CNESS 1999.

TABLE I. THE PARAMETERS OF RADARSAT-1/SAR FINE MODE PARAMETERS

Launching agency	Canadian Space Agency
Launching date	1995/11/04
Attitude	798km
Repeat cycle	24 days
Frequency	53GHz
Polarization	HH
Resolution	8m
Observation range	45km

TABLE II. THE PARAMETERS OF SPOT-2/HRV PARAMETERS

Launching agency	CNES
Launching date	202/05/4
Attitude	822km
Repeat cycle	26 days
Band width	Multi-spectral mode XS1 0.50-0.59 μ m XS2 0.61-0.68 μ m XS3 0.79-0.89 μ m
Resolution	5m
Observation range	60km

Copyright (c) IARIA, 2014. ISBN: 978-1-61208-354-4

$$D_P = a_1P + a_2L + a_3h + a_4 \quad (1)$$
$$D_L = b_1P + b_2L + b_3h + b_4. \quad (2)$$

Here, $D_P$and $D_L$are distortions of pixel and line directions, P and L denote coordinate values of pixel and line directions, respectively. Furthermore, h is the hight of area and $a_i, i = 1, 2, 3, 4$ and $b_i, i = 1, 2, 3, 4$ are regression coefficients.

IV. SOM ALGORITHM

We briefly summarize the algorithm for SOM. The structure of SOM consists of two layers. One is an input layer and the other is a competitive layer. The total input to a neuron j is denoted by net_j and modeled by the following equations:

$$\text{net}_j = \sum_i^n w_{ji}x_i = (w_{j1}, w_{j2}, \ldots, w_{jn})(x_1, x_2, \ldots, x_n)^t$$
$$= W_jX^t \quad (3)$$
$$W_j = (w_{j1}, w_{j2}, \ldots, w_{jn}),\ X = (x_1, x_2, \ldots, x_n) \quad (4)$$

where $(\cdot)^t$denotes the transpose of $(\cdot)$ and x_i and w_{ji} show an input in the input layer and a weighting function from the input x_i to a neuron j in the competitive layer, respectively. For simplicity, we assume that the norms of X and W_j are equalt to one, that is,

$$\|x\| = 1, \quad \|W_j\| = 1, j = 1, 2, \ldots, N \quad (5)$$

where $\|\cdot\|$ shows Eucridean norm and N denotes the total number of neurons in the competitive layer.

When an input vector X is applied to the input layer, we find the nearest neighboring weight vector W_c to the input vector X such that

$$\|W_c - X\| = \min_i \|W_i - X\|. \quad (6)$$

The neuron c corresponding to the weight vector W_c is called a winner neuron. We select neighborhood neurons within the distance d which are shown in Fig. 6 and a set of indices for neurons located in the neighborhood of c is denoted by N_c. Then, the weighting vectors of the neurons contained in N_c are changed such that those weighting vectors could become similar to the input vector X as close as possible. In other words, the weighting vectors are adjusted as follows:

$$\Delta W_j = \eta(t)(W_j - X) \qquad \forall j \in N_c \quad (7)$$
$$\Delta W_j = 0 \qquad \forall j \notin N_c \quad (8)$$

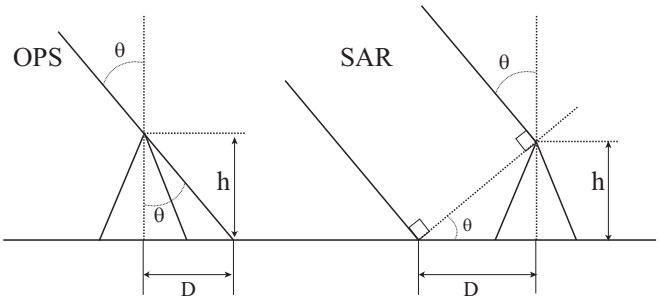

Figure 5. The principle of distortion of remote sensing data depending on the hights in case of optical sensory data and SAR data.

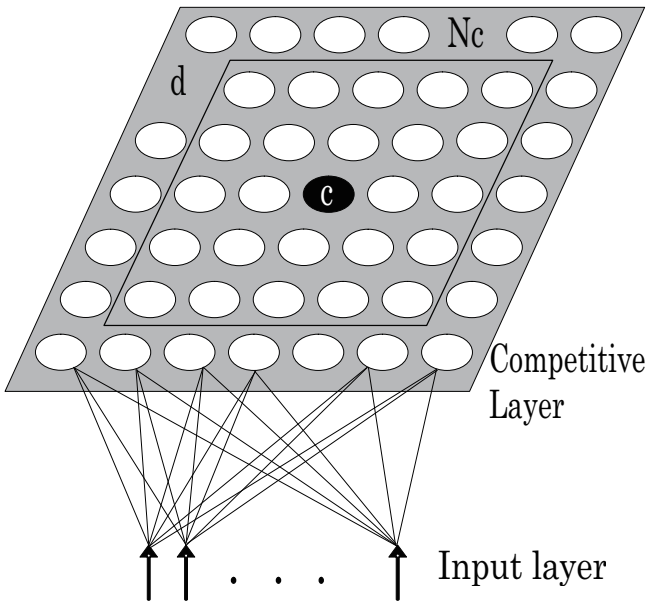

Figure 6. SOM structure of the neural network.

where

$$\Delta W_j = W_j(\text{new}) - W_j(\text{old}) \quad (9)$$
$$\eta(t) = \eta_0(1 - \frac{t}{T}), \qquad d(t) = d_0(1 - \frac{t}{T}). \quad (10)$$

Here, t and T denote an iteration number and the total iteration number for learning, respectively. η_0 and d_0 are positive and denote initial values of $\eta(t)$ and $d(t)$, respectively where $d(t)$ denotes an Euclid distance from the winner neuron c.

V. EVALUATION OF SOM

We will introduce two criteria, namely, precision and recall to find a suitable SOM. The precision is defined by

$$P_r = \frac{R}{N} \times 100(\%) \quad (11)$$

and the recall is defined by

$$R_r = \frac{R}{C} \times 100(\%) \quad (12)$$

where P_r and R_r denote the precision rate and the recall rate, respectively and N is a trial number, R is a correct classified number, and C is a total correct number. As shown in Fig. 7, if we try to increase P_r, then, R_r will decrease. Therefore, we adopt a criterion f-measure defined by

$$f_m = \frac{2 \times P_r \times R_r}{P_r + R_r} \times 100(\%). \quad (13)$$

VI. TRAINING OF SOM

In order to find a suitable size of competitive layer, we assume map size m as 3×3, 4×4, 5×5, 6×6, and 7×7. We take an initila learning rate α_0=0.2 and an initial value of neighborhood d_0=2. Furthermore, we assume initial values of connection weights as random numbers of [0.1, 0.9] and itelation number t=5. The training results of SOM are shown

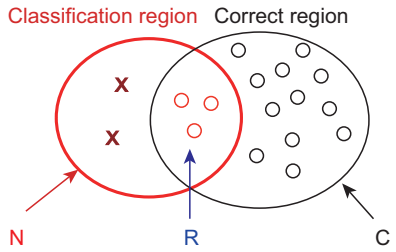

Figure 7. Classification region for the precision and the recall.

in Fig. 8 and Fig. 9 for SPOT remote sensing data and RADARSAT remote sensing data, respectively.

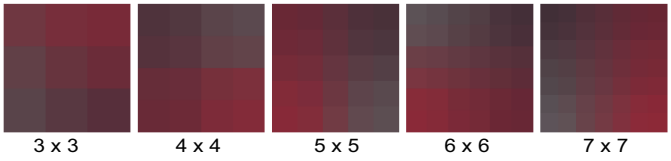

Figure 8. Learning results for SPOT remote sensing data.

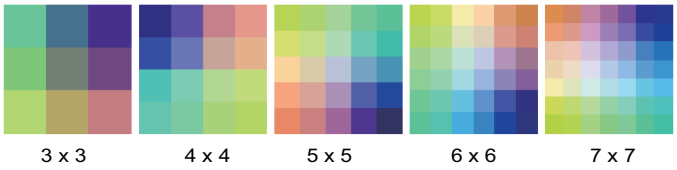

Figure 9. Learning results for RADARSAT remote sensing data

After taining the neural network of SOM, we calculate the P_r, R_r, and f_m for SPOT and RADARSAT remote sensing data. The results are shown in Table III and Table IV, respectively. From Table III, we can see that the classification result of the map size 4×4 is highest value of f_m=84.49. Thus, in case of a small number of category, we can set small number of neurons in the competitive layer. From Table IV, we can see that f_m becomes largest in case of 4×4.

TABLE III. P_r,R_r, AND f_m FOR SIZES OF SPOT REMOTE SENSING DATA

Size of map	P_r	R_r	f_m
3$times$3	98.95	64.67	78.22
4$times$4	100	73.15	84.49
5$times$5	93.62	76.65	84.29
6$times$6	85.65	68.65	76.21
7$times$7	96.16	63.00	76.13

TABLE IV. P_r,R_r, AND f_m FOR SIZES OF RADARSAT REMOTE SENSING DATA

Size of map	P_r	R_r	f_m
3$times$3	63.08	47.72	54.34
4$times$4	60.99	51.38	55.77
5$times$5	62.73	46.41	53.35
6$times$6	60.48	51.02	55.35
7$times$7	47.63	64.70	54.87

VII. SELECTION OF TRAINING ITERATION

We consider the iteration t for learning. Here, we count t=1when an input image of 1,800,000 pixels of 1,500pixels per line ×1,200 lines has been trained. In this experiment, we take t=1 (1,800,000 training), t=5 (9,000,000 training), t=10 (18,000,000 training), t=20 (36,000,000 training). Except for t, we take a size of neurons in the competitive layer as 4×4, α_0=0.2, and an initial vector W_0 of weighting functions are random numbers of [0.1, 0.9]. The results are shown in Table V and Table VI for SPOT and RADARSAT remote sensinr data, respectively.

TABLE V. P_r, R_r, AND f_m FOR ITERATIONS OF SPOT

Iteration	P_r	R_r	f_m
1	100	64.67	78.22
5	100	73.15	84.49
10	100	76.65	84.29
20	100	68.65	76.21

TABLE VI. THE VALUES OF P_r,R_r, AND f_m FOR ITERATIONS OF RADARSAT

Iteration	P_r	R_r	f_m
1	58.40	50.29	54.04
5	60.99	51.38	55.77
10	61.00	51.31	55.74
20	61.01	51.34	55.76

From Table V, we can see the maximum value of f_m=84.55 is obtained when t=5 for SPOT remote sensing data and from Table VI, the maximum value of f_m=55.77 is obtained when t=5. Therefore, we set t=5 in what follows.

VIII. CLASSIFICATION RESULTS

A rice-planted area was extracted by using SOM from three temporal RADARSAT images and one SPOT image. SOM is a classification method based on competitive neural networks without teacher. It was applied to the remote sensing data by using the parameters as shown in Table VII. RADARSAT and SPOT images were classified into 16 categories by SOM. Then, we labeled the categories into a rice-planted area, a forest area and an urban area.

IX. EXPERIMENTAL RESULTS AND DISCUSSION

In order to make the proposed method effective, we classify the satellite image data by SOM. Fig. 10 shows the classification image by SPOT and Fig. 11 shows the classification image by RADARSAT. By comparing Fig. 10 with Fig. 11, one can see that the rice-planted area by RADARSAT was extracted less than that by SPOT. The speckle noise was still seen in the image of rice-planted area, the majority filter with 7×7 window was applied to the rice extracted images by RADARSAT and SPOT. For the evaluation of the rice-planted area extraction, we defined two indices, True Production Rate (TPR) and False Production Rate (FPR). The TPR and FPR are calculated by

$$TPR = \frac{\alpha}{\alpha+\beta} \times 100 \quad (14)$$

$$FPR = \frac{\gamma}{\alpha+\gamma} \times 100 \quad (15)$$

where α means the number of relevant rice-planted area extracted, β means the number of relevant rice-planted area not

TABLE VII. THE PARAMETERS OF SOM

Neurons	Training iterations	η_0	d_0
4 × 4	1080,000	0.03	2

Copyright (c) IARIA, 2014. ISBN: 978-1-61208-354-4

extracted, and γmeans the number of irrelevant rice-planted area extracted. Extraction rice-planted area of SPOT image by supervised MLH was used as reference rice-planted area image.

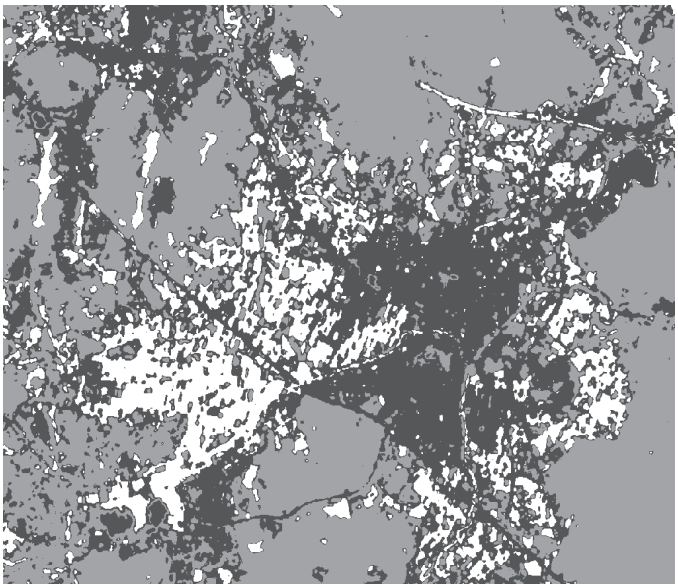

Figure 10. Classification result of SPOT image by SOM (White: rice, Light gray: forest, Dark gray: urban).

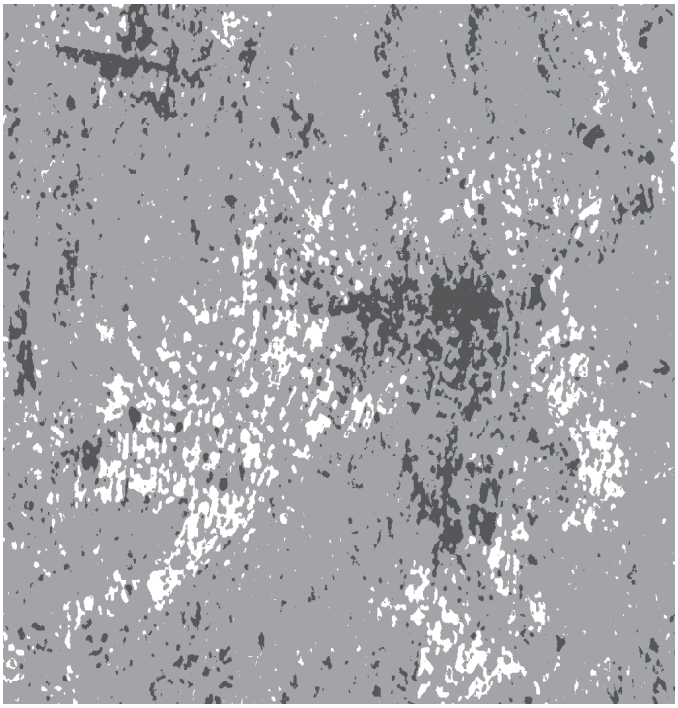

Figure 11. Classification result of RADARSAT image by SOM (White: rice, Light gray: forest, Dark gray: urban).

Table VIII shows the results of TPR and FPR by SOM and MLH classification for SPOT data and RADARSAT data. From this results we can see that in case of RADARSAT data, the values of TPR (extraction rate of rice-planted area) are, 50.97% and 60.96% for MLH and SOM, respectively. This means that SOM is better than MLH for extraction of rice-planted area by about 10%. As for FPR (misclassification rate) SOM is also better than MLH by about 3%. The SPOT data is very fine images like 5m per pixel and we can assume the image of SPOT reflects almost all land surface. Using SPOT data TPR and FPR are 70.41% and 21.51%, respectively. Thus, we could extract rice-planted area a certain level in practice fron Table VIII.

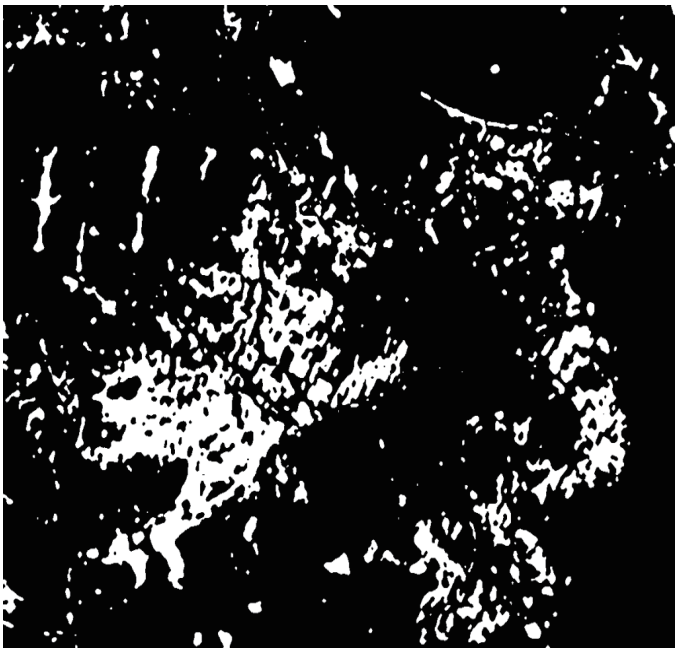

Figure 12. Extraction result of rice-planted area by SPOT data.

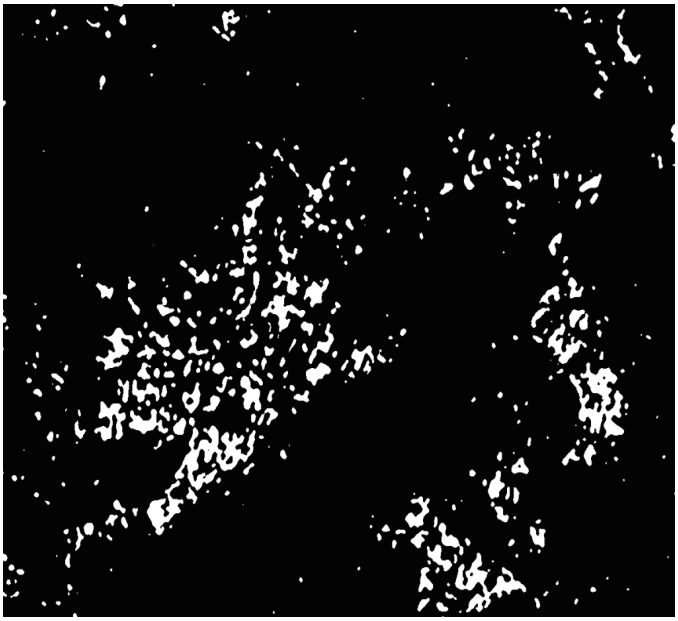

Figure 13. Extraction result of rice-planted area by multi temporal RADARSAT data.

Figs. 12 and 13 show the extraction result of rice-planted area by SPOT and RADARSAT, respectively. The results show that fine rice-planted area could be extracted by using SOM

compared with MLH from there figures.

TABLE VIII. THE RESULTS OF TPR AND FPR FOR RICE-PLANTED AREA EVALUATION

Comparison data	Classification method	TPR(%)	FPR(%)
SPOT	SOM	70.4	21.51
RADARSAT	MLH	50.97	51.44
RADARSAT	SOM	60.97	48.59

X. CONCLUSION AND FUTURE WORK

Rice-planted area extraction was attempted using multi-temporal RADARSAT data taken in an early stage of rice growing season by SOM classifications. The SOM is unsupervised classification whose computational time is shorter than the other supervised classification method like MLH [3] or LVQ [4][11]. We have been engaged with image analysis on remote sensing data analysis. Especially, we are concentrated on SAR data analysis to land cover classification by using neural network classification methods. Since the SAR data is completely different with optical sensor images, it is difficult to obtain usual land cover map although it can observe the earth at any time and under any weather conditions such as rainy or cloudy occasion. Thus, we must develop the special attention to get suitable classification results. In this paper, we have developed a method to allocate seasonal data to get the color image and show the change of rice field area in a visual way. It takes much time for extraction of features of SAR images, we must speed up the classification. we are now developing nearest neighbor algorithm. As for this results, we will show the results near future. The future study, we will apply this proposed and other neural network method to other SAR data due to the extraction rice-planted area. As we could obtain more high resolution images, we are checking the preset results for those big data and trying to make senario for them.

ACKNOWLEDGMENT

This work was supported by JSPS KAKENHI Grant-in-Aid for Challenging Exploratory Research (25630180). The authors would like to thank JSPS to support this research work.

REFERENCES

[1] Y. Suga, Y. Oguro, and S. Takeuchi, “Comparison of Various SAR Data for Vegetation Analysis over Hiroshima City”, *Advanced Space Research*, vol. 23, August, 1999, pp. 225–230.

[2] Y. Suga, S. Takeuchi, and Y. Oguro, “Monitoring of Rice-Planted Areas Using Space-borne SAR Data”, *Proceedings of IAPRS*, XXXIII, B7, February, 2000, pp. 741–743.

[3] S. Omatu, “Rice-Planted Areas Extraction by RADARSAT Data Using Learning Vector Quantization Algorithm”, *Proceedings of ADVCOMP 2013*, Sep., 2013, pp. 19–233.

[4] T. Konishi, S. Omatu, and Y. Suga, “Extraction of Rice-Planted Areas Using a Self-Organizing Feature Map ”, *Artificial Life and Robotics*, 2007, vol. 11, pp. 215–218.

[5] I. H. Woodhouse, *Introduction to Microwave Remote Sensing*. CRC Press, London, Nov. 2005, ISBN: 0-415-27123-1.

[6] C. M. Ryan, T. Hill, E. Woollen, C. Ghee, E. Mitchard, G. Cassells, J. Grace, I. H. Woodhouse, and M. Williams, “Quantifying Small-Scale Deforestation and Forest Degradation in African Woodlands Using Radar Imagery ”, *Global Change Biology*, vol. 18, pp. 243–257, 2012 ISSN: 1365-2486.

[7] E. T. A. Mitchard, S. S. Saatchi, L. J. T. White, K. A. Abernethy, K. J.Jeffery, S. L.Lewis, M. Collins, M. A.Lefsky, M. E. Leal, I. H. Woodhouse, and P. Meir, “Mapping Tropical Forest Biomass with Radar and Spaceborne LiDAR in Lope National Park, Gabon: Overcoming Problems of High Biomass and Persistent Cloud”, *Biogeosciences*, vol. 9, pp. 179-191, 2012, doi: 10.5194/bg-9-179-2012.

[8] C. H. Chen, Ed.,*Signal and Image Processing*, London, Jan. 2007, chapter 27, pp. 607–619, M. Yoshioka, T. Fujinaka, and S. Omatu,*SAR Image Classification by Support Vector Machine* , ISBN: 0-8493-5091-3.

[9] M. Bicego and T. L. Toan, “Rice Field Mapping and Monitoring with RADARSAT Data”, *International Journal of Remote Sensing*, vol. 20, April, 1999, pp. 745–765.

[10] S. C. Liew, and P. Chen, “Monitoring Changes in Rice Cropping System Using Space-borne SAR Imagery”, *Proceedings of IGARSA’99*, Oct., 1999, pp. 741–743.

[11] T. Kohonen, “Self-Organizing Maps”, *Springer*, 1997, pp. 206–217, ISBN 3-540-62017-6.

Copyright (c) IARIA, 2014. ISBN: 978-1-61208-354-4